Intradermal delivery of an immunomodulator for basal cell carcinoma; expanding the mechanistic insight in solid microneedle enhanced delivery of hydrophobic molecules

Akmal Sabri, [†] *Jane Ogilvie,* [‡] *John McKenna,* [§] *Joel Segal,* [∥] *David Scurr,* [†] *and Maria Marlow* [*, †]

[†] School of Pharmacy, University of Nottingham, Nottingham NG72RD, United Kingdom.

[‡] Walgreens Boots Alliance, Thane Road, Nottingham, NG90 1BS

[§] Leicester Royal Infirmary University Hospitals Leicester Dermatology Department, Infirmary Square, Leicester LE1 5WW

[∥] Department of Mechanical, Materials and Manufacturing Engineering, Faculty of Engineering, University of Nottingham, Nottingham, NG8 1BB

KEYWORDS: Microneedles, imiquimod, basal cell carcinoma, time-of-flight secondary ion mass spectrometry.

ABSTRACT

Basal cell carcinoma (BCC) is the most common cutaneous malignancy in humans. One of the most efficacious drugs used in the management of basal cell carcinoma BCC is the immunomodulator, imiquimod. However, imiquimod has physiochemical properties that limit its permeation to reach deeper, nodular tumour lesions. The use of microneedles may overcome such limitations and promote intradermal drug delivery. The current work evaluates the effectiveness of using an oscillating microneedle device Dermapen® either as a pre or post-treatment with 5% w/w imiquimod cream application to deliver the drug into the dermis. The effectiveness of microneedles to enhance the permeation of imiquimod was evaluated *ex vivo* using a Franz cell set up. After a 24-hour permeation experiment, sequential tape strips and vertical cross-sections of the porcine skin were collected and analysed using time-of-flight secondary ion mass spectrometry (ToF-SIMS). In addition, respective Franz cell components were analysed using high performance liquid chromatography (HPLC). Analysis of porcine skin cross-sections demonstrated limited dermal permeation of 5% w/w imiquimod cream. Similarly, limited dermal permeation was also seen when 5% w/w imiquimod cream was applied to the skin that was pre-treated with the Dermapen®, this is known as poke-and-patch. In contrast, when the formulation was applied first to the skin prior to Dermapen® application, this is known as patch-and-poke, we observed a significant increase in intradermal permeation of imiquimod. Such enhancement occurs immediately upon microneedle application, generating an intradermal depot that persists for up to 24 hours. Intradermal colocalization of isostearic acid, an excipient in the cream, with imiquimod within microneedle channels was also demonstrated. However, such enhancement in intradermal delivery of imiquimod was not observed when the patch-and-poke strategy used a non-oscillating

microneedle applicator, the Dermastamp^{TM}. The current work highlights that using the patch-and-poke approach with an oscillating microneedle pen may be a viable approach to improve the current treatment in BCC patients who would prefer a less invasive intervention relative to surgery.

1. Introduction

Basal cell carcinoma (BCC) is the most common skin cancer in humans [1]. Despite having a low tendency to metastasize, BCC may result in substantial peripheral tissue destruction if left untreated [2]. The two most common BCC subtypes are superficial and nodular [3]. Superficial BCC generally manifests and proliferates parallel to the epidermis [4,5]. On the other hand, nodular BCC typically resides deep within the papillary and reticular dermis [6]. Despite the effectiveness of surgical interventions which display a 95% cure rate [7], accurate detection of tumour margins prior to surgery is pivotal in ensuring complete tumour resection. Such prerequisites are both time-consuming and technical, which limits the use of such treatments [8]. In addition, not all BCC patients are suitable for surgical intervention and some may opt for non-surgical treatment due to lower overall cost and better cosmetic outcomes [9-10]. This is further corroborated by the findings of Tinelli *et al* who reported that patients generally preferred topical therapy over surgical intervention [11]. One of the most efficacious drugs used in topical therapy for BCC is the immunomodulator, imiquimod [12].

Recently, William *et al* reported that topical imiquimod therapy for BCC resulted in a cure rate significantly less than surgical intervention [13]. The lower cure rate of imiquimod in treating BCC, particularly the nodular variant is due to the location of the tumour that resides deeper within the dermis [14]. This tumour location provides an anatomical barrier for imiquimod to permeate in sufficient quantity to eradicate the tumour [15].

One of the methods to improve the delivery of therapeutics for the treatment of BCC is via the use of microneedles. Microneedles are biomedical devices that consist of arrays of fine needles with lengths ranging between 250 and 1000 μm. Upon application to the skin, these devices generate transient channels that provide a route across the *stratum corneum* into the deeper layers of the skin [16]. The application of microneedle-based drug delivery for the management of BCC was pioneered by Donnelly *et al* [17]. Donnelly *et al* demonstrated that microneedles enhanced the localised delivery of aminolaevulinic acid into the skin for BCC treatment. Further to this Naguib *et al.* demonstrated, via a murine model, the feasibility of using solid microneedles to enhance the intradermal delivery of 5-fluorouracil to treat skin tumours. Following these studies, various groups have explored different microneedle designs to deliver a range of anticancer agents such as methyl aminolevulinic acid (MAL) [18], meso-tetra(N-methyl-4-pyridyl)orphinetetratosylate (TMP) [19], and itraconazole [20].

Detailed analysis of the dermal distribution of pharmaceuticals within the skin strata is paramount in order to evaluate the permeation enhancement effect conferred by microneedles for targeted skin delivery. Traditionally, chromatographic analysis (e.g. high-performance liquid chromatography, HPLC) is frequently implemented in microneedle permeation studies in order to evaluate the delivery of drugs into and across the skin. However, this analytical method is dependent on efficient drug extraction and effective column separation from co-extracted endogenous components of the skin. Furthermore, the tissue manipulation steps and extraction procedures lead to the loss of valuable spatial information regarding drug localisation within the skin tissue [21]. In order to overcome this limitation, microneedle permeation studies frequently use fluorescently-tagged molecules in order to track their distribution within the skin [22]. This method of tracking dermal distribution can be achieved via the use of confocal laser scanning microscopy

(CLSM). CLSM utilises point illumination via the use focused laser beam that is rastered across the sample of interest. The emitted fluorescence from the in-focus plane is passed through a pinhole onto a detector, which the measures the fluorescence from the site of analysis. Any out-of-focus fluorescence is blocked by the pinhole, which is said to be confocal with the focal point of the objective lens. CLSM has been used to tracked the permeation of compounds delivered using microneedle-based delivery systems [23–25]. Although this approach allows the experimenters to track drug localisation within the skin, the use of fluorescent tagging with this method alters the physiochemical properties of molecules leading to erroneous estimation of drug distribution in biological tissues [26]. In addition, the need for different fluorescent tagging to track the dermal distribution of multiple molecules complicates the method even further. Hence, there is a clear need for advanced analytical techniques to be utilised in the field of microneedle research to allow researchers to track drug distribution within skin tissues in a label-free manner.

Some of the techniques that offer label-free imaging of dermal drug distribution include confocal Raman microscopy and stimulated Raman scattering microscopy. These techniques has been used to visualise the dermal distribution of several pharmaceuticals such as 5-fluorouracil [27], ketoprofen [28], and terbinafine [28]. Although these methods offer experimenters the ability to visualise dermal drug distribution in a label-free manner, the Raman signal is normally a weak. This necessitates that the molecule of interest should be present at sufficient concentration to allow detection. In addition, the drug molecules also need to possess Raman active chemical groups that are different from native skin biomolecules to permit differentiation and detection. Another issue associated with Raman-based imaging is the high level of autofluorescence from biological tissue which can mask the weak Raman signal thus limiting the utility of these techniques to map dermal drug distribution [29].

Time-of-flight secondary ion mass spectrometry (ToF-SIMS) on the other hand is a powerful surface analytical technique that confers excellent mass and spatial resolution along with chemical sensitivity [30,31]. Analysis of samples using ToF-SIMS allows chemical mapping of the distribution of a compound of interest by tracking the mass-to-charge ratio (*m/z*) of specific molecular ions from the mass spectra. This analytical approach allows us to track the distribution of compounds, both exogenous and endogenous, within a biological milieu in a label-free manner. Such analytical power conferred by ToF-SIMS has led to the use of the technique to analyse a range of biological materials such as insulin and even cancerous tissue [32–37]. In addition, the ability of the instrument to track the topical permeation of pharmaceuticals and cosmeceuticals such as chlorhexidine [38,39], ascorbic acid [21], dihydroquercetin [40], fatty acids [41], carvacrol [42] and roflumilast [43] highlights the value of the technique in skin research. Despite the powerful analytical capability offered by this form of mass spectrometry imaging, the utility of ToF-SIMS in evaluating the effectiveness of microneedle-based drug delivery system has yet to be fully demonstrated.

A previous study demonstrated the limited permeation of imiquimod into the skin when the drug is administered as a topical cream [44]. This work also demonstrated that solid microneedles provided a solution to deliver imiquimod beyond the *stratum corneum* and into the viable epidermis. However, such delivery depth was not sufficient to reach the dermal depth in which nodular BCC typically resides. In the present work, we explore further the application of solid microneedles as a physical permeation enhancement strategy to deliver imiquimod deeper into the dermis for BCC treatment. In addition, the microneedle system should deliver imiquimod to a depth of approximately 400 μm below the skin surface which is the target region in which nodular BCC typically manifests [13]. The current study highlights that the approach in which microneedles are used in combination with an imiquimod cream, can lead to the successful intradermal delivery of

imiquimod. The concept of using a patch-and-poke strategy with solid microneedles was initially conceptualized in a review published by McCaffrey *et al.* as a method to deliver genes into the skin [45]. Patch-and-poke is defined at the application of formulations onto the skin prior to solid microneedle application. However, research on the effectiveness of the patch-and-poke approach using solid microneedle is limited. This is because research on solid microneedles focuses mostly on a poke-and-patch strategy to deliver drug into or across the skin. Furthermore, using the poke-and-patch strategy results in the generation of hydrophilic/aqueous microneedle channels post application that act as a barrier to the permeation of hydrophobic drugs into the skin [46,47]. Therefore, there is a lacuna in the knowledge about the effectiveness of using the patch-and-poke approach with solid microneedles.

In this work, it is demonstrated that a patch-and-poke strategy is more effective in delivering imiquimod intradermally than the conventional poke-and-patch approach. This work also demonstrated that microneedle oscillation during application plays an important role in the effective intradermal delivery of imiquimod using the patch-and-poke strategy.

2. Experimental section

2.1. Materials

Imiquimod was purchased from Cayman Chemicals, USA. Aldara™ topical cream (5% w/w imiquimiod), MEDA Company, Sweden was purchased from Manor pharmacy, UK. Dermapen®, which is a microneedling pen, was purchased from ZJchao, China. The microneedles on the Dermapen® had a tapered conical structure. The microneedle had a base diameter of 370 μm with a tip radius of 53.4º. The distance between microneedles (pitch) was 620 μm. Microneedles were arranged in rows which formed an overall circular area. The Dermapen® has five different oscillation speeds- 8000, 10000, 12000, 14000 and 16000 RPM. In addition, the needle length

could be adjusted between 250-1500 µm. For the purpose of the permeation study, we selected a microneedle length 1000 µm and an oscillation speed of 8000 RPM. During application, the pen was held by one hand with gentle pressure while the hand was used to hold the skin in place. The Dermastamp™ which was a microneedle stamp, was purchased from Teoxy Beauty, Wuhan, China. The microneedles on the Dermastamp™ also had a tapered conical structure. The microneedle had a base diameter of 210 µm with a tip radius of 22.8º. The distance between microneedles (pitch) was 1050 µm. Microneedles were arranged in an annular fashion which formed an overall circular area. The Dermastamp™ had no oscillating function and the needle length of the Dermastamp used was fixed to 1000 µm. During application, the Dermastamp™ was held by one hand with and applied by one swift stamping motion with gentle pressure. Sodium acetate was purchased from Sigma-Aldrich, UK. Acetonitrile (HPLC grade) and glacial acetic acid were obtained from Fisher Scientific, UK. Teepol solution (Multipurpose detergent) was ordered from Scientific Laboratory Supplies, UK. D-Squame standard sampling discs (adhesive discs) were ordered from Cuderm corporation, USA. OCT media was obtained from VWR International Ltd. Belgium. Deionised water was obtained from an ELGA reservoir, PURELAB® Ultra, ELGA, UK. All reagents were of analytical grade, unless otherwise stated. *Ex vivo p*orcine skin was used to investigate the permeation of imiquimod due to the similarities in histology, thickness and permeability to human skin [48]. Skin samples were prepared from ears of six month old pigs obtained from a local abattoir prior to steam cleaning. Full skin thickness was used to prevent altering the skin biomechanical properties which may lead to over-penetration of the microneedles into the skin [49]. The porcine skin samples were stored at -20 °C until analysis. The integrity of the skin samples prepared via this method was assessed by electrical resistance, using the method and guidelines described by Davies *et al* using EVOM2 Voltohmmeter (World Precision Instruments,

U.S.A). Only skin that produced an electrical resistance reading of greater than 10 kΩ was used. [50].

2.2.1. Permeation study of 5% w/w imiquimod cream through porcine skin

Imiquimod dermal permeation with and without microneedle treatment was evaluated *ex vivo* using a Franz-type diffusion cell. Prior to the permeation study, skin samples were defrosted for at least an hour at room temperature. The skin was trimmed into small pieces according to the surface area of the donor chamber of the Franz diffusion cell (Soham Scientific, Cambridgeshire, UK). The trimmed skin samples were equilibrated by placing them above the receptor compartment for 15 minutes prior to skin treatment. The Franz cells used in this study has a receptor compartment volume of 3 ml.

The porcine skins were subjected to the following treatment modalities: i) application of 20 mg Aldara™ cream alone ii) application of 1000 µm microneedles to the skin as a pre-treatment using Dermapen® followed by 20 mg Aldara™ cream. 1000 µm refers to the length of the microneedles. This is known as the poke-and-patch approach. 12-microneedle array cartridges were used for this treatment. iii) Application of 20 mg Aldara™ cream followed by 1000 µm microneedle treatment using Dermapen®. This is known as the patch-and-poke approach. Either a 12-microneedle or a 36-microneedle array cartridge were used for this treatment. All the arrays used in the microneedle treatment groups have similar surface area of application which is 0.64 cm^2

Next, the porcine skins were placed on top of the receptor compartment filled with 3 ml of degassed 100 mM acetate buffer pH 3.7. This buffer was selected as the receptor phase in order to maintain a sink condition throughout the permeation study. This is due to the insolubility of imiquimod at neutral or basic pH values. Various groups have reported the use of acetate buffer pH 3.7 as the receptor phase in imiquimod permeation studies [51–53]. The skin was then secured between the donor

and receptor compartment of the diffusion cell using a metal clamp, with the stratum corneum side facing the donor compartment. Upon assembling the Franz diffusion cell, the permeation experiment was conducted over a period of 24 hours in a thermostatically controlled water bath set at 36.5 ^{o}C.

2.2.2 Quantification of imiquimod post-permeation study

After a 24-hour permeation experiment, the excess cream was removed and collected from the skin surface by careful application of sponges soaked with 3% v/v Teepol® solution. The sponges were pooled for imiquimod HPLC analysis as a total skin wash. Any formulation which might have spread to the donor chamber was collected by the sponges and stored for imiquimod analysis by HPLC as a donor chamber wash. Upon removing excess formulation from the skin surface, 15 sequential tape strips were collected from the skin as detailed in Section 2.2.4.

The amount of imiquimod from the different Franz cell elements (skin wash, donor chamber wash, pooled tape strips and remaining skin after tape stripping) were extracted by the addition of 5, 5, 10 and 5 mL of methanol extraction mixture (Methanol 70%: Acetate Buffer pH 3.7 100 mM 30%) respectively using a previously reported method [54]. Samples were then vortexed for 1 minute and sonicated for 30 minutes before being left overnight. Subsequently, samples were vortexed again and sonicated for a further 30 minutes. 1 ml of the extracts were collected and spiked with 100 µl of 100 µg/ml propranolol as an internal standard. The samples were then filtered through 0.22 µm membrane. For the receptor fluid, 1 ml of the solution from each Franz cells were collected and spiked with 100 µl of 100 µg/ml propranolol as an internal standard before being filtered through 0.22 µm membrane. HPLC analysis was carried out using an Agilent 1100 series instrument (Agilent Technologies, Germany) equipped with degasser, quaternary pump, column thermostat, autosampler and UV detector. System control and data acquisition were performed using

Chemostation software. The details of the HPLC chromatographic conditions are as follow: column C18 (150 × 4.6 mm) ACE3/ACE-HPLC Hichrom Limited, UK. The mobile phase composition for analysis of extracts from skin wash, donor chamber wash, pooled tape strips and remaining skin consists of 10 mM acetate buffer: acetonitrile (79:21). Whilst, the mobile phase composition for analysis of receptor fluid consists of 10 mM acetate buffer: acetonitrile (70:30). The system operated at a flow rate of 1.0 mL/minute, UV detection at λ max=226 nm, injection volume of 40 µL and column temperature of 25 °C.

2.2.3 Tape stripping and cryo-sectioning of porcine skin post-permeation experiment for ToF-SIMS analysis.

After 24 hours, the skins were detached from the Franz diffusion cells. Excess Aldara^{TM} cream was removed. 15 sequential tape strips were collected for each skin samples. Sequential removal of corneocytes was judged by the resistance felt during the stripping step and the change in opacity of the tape post stripping. The skin was rotated 180° for each tape strip. This ensures that the tape stripping would not result in premature removal of the whole *stratum corneum* during tape stripping. All tape strips collected were stored in a freezer at -20 °C until analysis.

In order to measure the depth of imiquimod permeation into the skin, the permeation experiments were repeated as described above in Section 2.2.2. After the permeation study, excess formulation was removed and a 1 cm x 1 cm of each microneedle application site was fresh frozen with liquid nitrogen. Skin cross-sectioning was performed using a cryostat (Leica CM3050 S Research Cryostat, UK). The skin slices were then thaw mounted on a glass slides and stored at -20 ºC prior to ToF-SIMS analysis.

2.2.4 ToF-SIMS analysis

ToF-SIMS was used to analyse individual tape strips and cryo-sectioned porcine skin samples. ToF-SIMS analysis was performed using a ToF-SIMS IV instrument (IONTOF, GmbH) with a Bi_3^+ cluster source. A primary ion energy of 25 KeV was used, the primary ion dose was preserved below 1×10^{12} per cm^2 to ensure static conditions. Pulsed target current of approximately 0.3 pA, and post-acceleration energy of 10 keV were employed throughout the sample analysis. The mass resolution for the instrument was 7000 at *m/z* 28. The scanned area of the tape strips samples was (4 mm × 4 mm) encompassing the skin area exposed to Aldara™ cream during Franz cell diffusion experiments. Whilst, an analysis area of (1.5 mm x 3 mm) was employed for the skin cross-sections. Both sample types were analysed at a resolution of 100 pixels/mm. An ion representing biological material and therefore indicative of skin (skin marker) was identified as CH_4N^+ and was used to threshold the data sets from tape strips. CH_4N^+ is a common fragment observed in organic materials such as biological specimens. Therefore, this secondary ion was used to track the presence of corneocyte extracted on the tape strips. The data was reconstructed to remove the data from the adhesive tape material found between the fissures in the stripped skin and therefore the data was only analysed from the skin material. Following this, each image of the individual tape strip (4 mm × 4 mm) was divided into four smaller data sets of (2 mm × 2 mm) which results in four repeats (n = 4) for each sample and their intensities were normalised to the total ion intensity. All ToF-SIMS data were acquired in positive spectra as this gave the best ionization intensity for imiquimod based on our previous work [44]. In addition, pure imiquimod, pure isostearic acid and Aldara™ cream reference spectra were obtained by analysing the pure drug, pure fatty acid and the cream on silicon wafers using ToF-SIMS.

2.2.5 Understanding the effect of vibration of Dermapen® on the intradermal permeation of imiquimod

One of the features of the Dermapen® is the ability of the device to vibrate the microneedles at the tip of the device. In order to understand the role of oscillation on the intradermal delivery of imiquimod into the skin, the permeation study was repeated as detailed in Section 2.2.2. However, porcine skins were subjected to the following treatment modalities: i) Application of 20 mg Aldara™ cream followed by 1000 µm microneedle treatment using Dermapen®. A 36-microneedle array cartridge was used for this treatment ii) Application of 20 mg Aldara™ cream followed by 1000 µm microneedle treatment using a non-vibrating Dermastamp™. The Dermastamp™ consists of 40-microneedle array per stamp. The Dermastamp™ was similar to the Dermapen® in terms of microneedle length used (which is 1000 µm) and the material used to manufacture the needle, which was stainless steel. The only main difference was that the Dermastamp™ did not have any vibration function. After a 24-hour permeation study, the skin samples were cryo-sectioned and analysed by ToF-SIMS using the same conditions outlined in Section 2.2.5. In addition, a time point study (0, 1, 6, 12 and 24 hours) was conducted to evaluate how the dermal distribution of imiquimod changes over the course of 24 hours with the patch-and-poke approach using the Dermapen®.

3. Results and discussion

3.1. Skin insertion and dye binding study

An *ex vivo* skin insertion study was conducted to establish the microneedle length needed to reach the skin strata where nodular BCC typically resides. From the supplementary data, **Figure S1**, it can be seen that when the length of Dermapen was adjusted to 1000 µm, an insertion depth of approximately 600 µm was observed. Such penetration depth is sufficient to reach beyond the epidermis layer and into the dermis layers. As nodular BCC typically manifests from the *stratum basale* at the dermoepidermal junction and grows deeper into the dermis, this suggests that

adjusting the Dermapen® to 1000 μm would provide sufficient penetration to reach nodular BCC tumours [55]. Therefore, guided by the skin insertion study data, we selected the 1000 μm length microneedles (Dermapen®) for the skin permeation study.

3.2 HPLC analysis of imiquimod from Franz cell components post-permeation study.

HPLC analysis was performed in order to quantify the amount of imiquimod that has remained or permeated into respective Franz cell compartments over the course of the permeation study. The mean amount of imiquimod (μg) recovered from the various Franz cell components following the 24-hour permeation study is shown in **Figure 1**. The amount of imiquimod extracted from the applied dose from cream alone was highest in the skin wash relative to other Franz cell components. This suggests that when imiquimod is delivered as a topical cream, the drug displayed limited permeation into the skin. Such findings agree with previous work that showed that application of imiquimod as a topical cream resulted in the majority of the dose being recovered from the skin surface [44]. However, the amount of imiquimod recovered contradicts the finding by Stein *et al,* who found that only 19% of the applied Aldara™ cream remained on the skin surface highlighting sufficient dermal permeation of imiquimod [56]. Such enhanced permeation reported by Stein and co-worker is likely due to the use of murine skin which is more permeable and thinner in comparison to human and porcine skin [57].

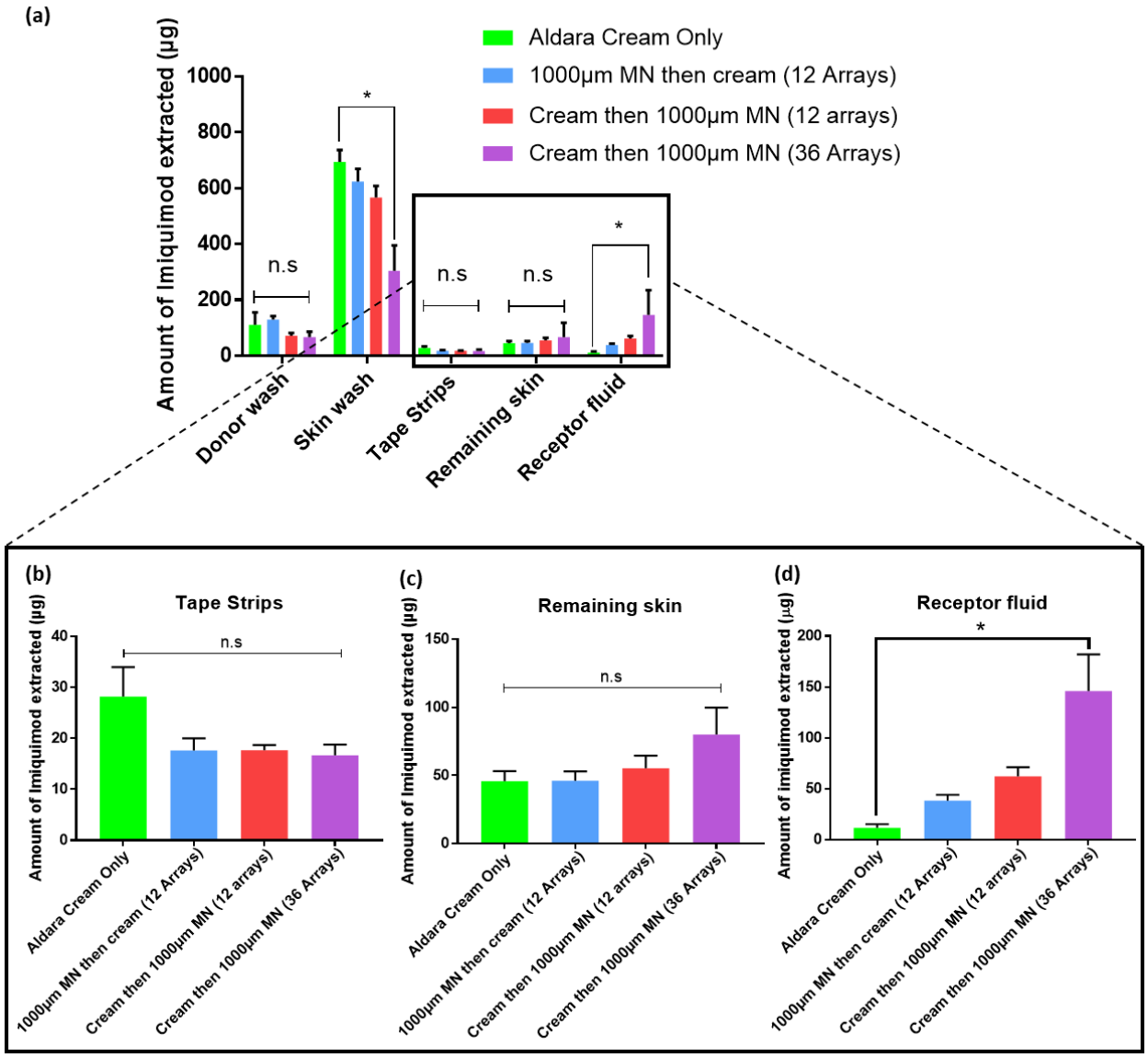

Figure 1 HPLC analysis of the mean amount of imiquimod recovered from the different Franz cell components (donor chamber wash, skin wash, tape strips, remaining skin and receptor fluid) post-permeation study. Data is presented as the mean ± SD (n = 6). The inset details the amount of imiquimod that has permeated into (b) tape strips (c) remaining skin and (d) receptor fluid. Differences were calculated using one-way ANOVA, followed by Tukey's post hoc test, and deemed significant at $p<0.05$. *n.s* = not statistically significant at $p>0.05$

One of the ways to circumvent the limited dermal permeation of imiquimod is to utilise a physical permeation enhancer such as microneedles to promote the delivery of the drug into the skin. Thus, in this study, we utilised a microneedling device, Dermapen® in order to enhanced imiquimod delivery into the skin. One of the earliest and simplest microneedle-based approaches to promote intradermal drug delivery is via the poke-and-patch method [46]. However, when we conducted an *ex vivo* skin permeation study, we observed that the delivery profile of imiquimod with the poke-and-patch approach was similar to topical cream application as shown in **Figure 1**.

One of the possible explanations for the similar permeation profile of imiquimod into and across *ex vivo* skin between these two strategies (cream alone vs poke-and-patch) is due to the formation of hydrophilic microneedle channels from the outflow of dermal interstitial fluid upon microneedle application [46,47]. Such channels may act as a barrier for the effective permeation of a hydrophobic drug such as imiquimod [58]. Therefore, we also investigated if the application of topical Aldara™ cream (5% w/w imiquimod) followed by microneedling, a patch-and-poke approach, as an alternative strategy to improve the delivery of imiquimod into the skin. When the *ex vivo* skin permeation study was carried out using the patch-and-poke strategy, we observed a decrease in the amount of imiquimod recovered from the skin wash. This was statistically significant when the patch-and-poke approach used a 36-needle cartridge.

Although not statistically significant, the HPLC analysis of imiquimod extracted from remaining skin showed an increasing trend in the amount of imiquimod delivered into the skin with the patch-and-poke approach in comparison to the poke-and-patch approach. However, the difference in the amount delivered across the skin was most prominent from the analysis of receptor fluid. Analysis

of receptor fluid indicates an increase in the amount of imiquimod delivered into and across the skin. However, such differences were only statistically significant when the patch-and-poke approach was adopted using the 36-microneedle array Dermapen®.

In addition, we have established that sink condition were maintained throughout our study as will be described. The saturation solubility of imiquimod, which is a weak base, in the receptor compartment, acetate buffer 100 mM, has been reported by De Paula *et al* is 1360.2 (μg/mL) at pH 4.0 [54]. Therefore, as we used a lower pH acetate buffer, pH 3.7, which has been used in by other investigators [51–53], we predicted that the solubility of the drug at pH 3.7 would be comparable if not higher than that reported by De Paula *et al*. Data for the receptor fluid that has been converted into μg/mL in the Supplementary Information (**Figure S2**) indicates that the highest concentration detected was on average 48.7 μg/ml. This indicates that after 24 hours, the highest average concentration imiquimod within the receptor fluid was 3% of its saturation solubility concentration reported. Ng *et al* have indicated that in order for sink conditions to be maintained, the penetrant concentrations in the receptor solution should not be more than 10% of their saturation solubility concentration [59]. Based on this information, we can confirm that sink conditions were indeed maintained throughout the permeation study.

The increase in amount of imiquimod delivered across into the receptor fluid may be attributed to the enhanced amount of imiquimod delivered into the dermis using the patch and poke approach. Imiquimod is known to have low aqueous solubility such as in the interstitial fluid within the dermal microenvironment, but displays higher solubility in acidic pH due the molecule being a weak base [54]. Based on the physiochemical property of the drug, it is likely that imiquimod delivered into the dermis may have partitioned into the acidic acetate buffer within the receptor solution over time as the drug has higher solubility in the acidic buffer. In addition, it is worth

noting that the dermis receives a rich blood supply that is derived from the hypodermis. Therefore, it is postulated that any drug that reaches this layer of the skin, after traversing the tortuous epidermal layers, has the potential to be rapidly absorbed into the systemic circulation [55]. Based on **Figure 1 (c)** and **(d)**, it can be inferred that the patch-and-poke strategy may result in improved delivery into the dermis which is target region for nodular BCC. The partitioning of the drug into the receptor fluid may provide some indication of potential systemic exposure. Based on **Figure 1** it can be inferred that although the patch-and-poke strategy may result in improved delivery into the dermis, such mode of delivery may lead to increased systemic exposure of imiquimod which could result is side effects such as flu-like symptoms [60]. However, such mode of delivery may lead to unwanted systemic exposure. Therefore, in order to limit the likelihood of such side effects arising, it could be suggested that reducing dosing frequency for the patch-and-poke strategy relative to the dosing frequency of Aldara™ application alone may mitigate the likelihood of such side effects arising.

3.3 ToF-SIMS analysis of tape strips post-permeation study

Despite HPLC analysis of different Franz cell component providing quantitative results, the method does not confer any information detailing imiquimod distribution within individual layers of skin. Therefore, an additional analytical technique was used to provide spatial information regarding imiquimod permeation. Analysis of samples using ToF-SIMS allows a chemical map of the distribution of a compound of interest to be acquired as well as providing information on how such distribution changes with depth. In previous work, it has been found that the permeation of the imiquimod across the skin could be tracked by monitoring the molecular ion $C_{14}H_{17}N_4^+$ [44]. ToF-SIMS secondary ion images of the analysed tape stripped area, which represents the exposed area of the skin to Aldara™ cream during Franz cell diffusion experiment, are illustrated in **Figure 2**. An ion representative of skin tissue (CH_4N^+) and a diagnostic imiquimod ion ($C_{14}H_{17}N_4^+$) ion images for tape strips no. 6 are shown in **Figure 2 (a)**. It was apparent that the signal from the skin marker (CH_4N^+) was much lower in the two top ion images. However, should there be a reduction or increase in the ions collected, each ToF-SIMS image collected is normalised to the total ion collected. As all the ion images collected have been scaled to the same value as shown with scale bars, we attributed the signal reduction from the skin marker (CH_4N^+) for the two top ion images is due to biological variation as the porcine skin used is from different pigs' ears.

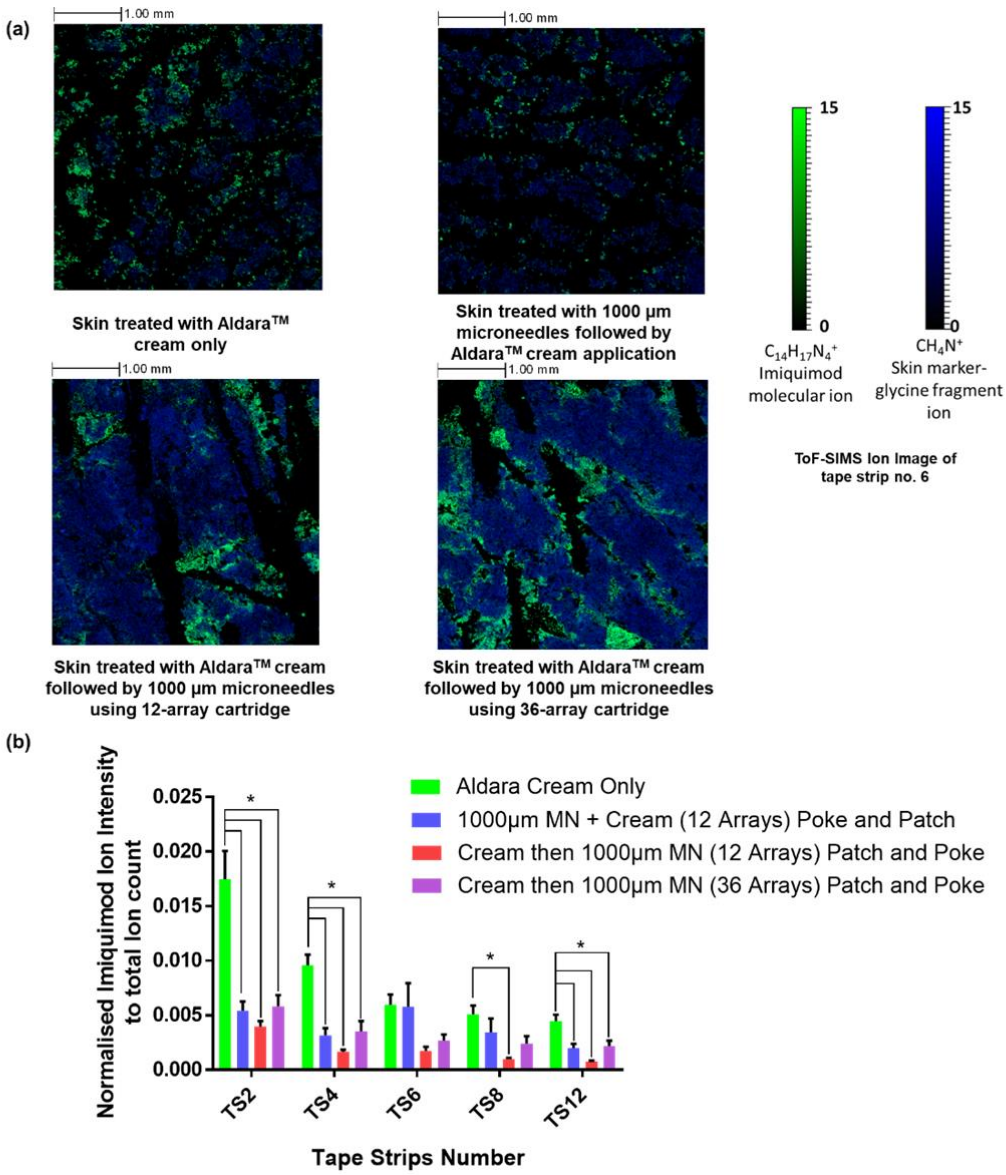

Figure 2. (a) ToF-SIMS 4 mm × 4 mm secondary ion distribution maps on tape strip surfaces. The scale bar represents 1 mm, and the images have been normalized to the total ion image. The distribution maps are from tape strip no. 6, showing the distribution of the imiquimod molecular ion ($C_{14}H_{17}N_4^+$), and biological marker for corneocytes (CH_4N^+) (b) ToF-SIMS exported peak intensities (normalized to total ion intensity) for imiquimod molecular ion peak as a function of increasing tape strip number from porcine skin. The skin was either treated with Aldara™ cream only, pre-treated with microneedles (1000 µm) before Aldara™ cream application or treated with

microneedles (1000 μm) of different array size after cream application. Data are expressed as mean ± SEM for n=12 analytical repeats. *MN*-refers to microneedles, Differences were calculated using one-way ANOVA, followed by Tukey's post hoc test, and deemed significant at $p<0.05$

Figure 2 (b) highlights how imiquimod ion intensity changes with *stratum corneum* depth as a function of tape strip number. The decrease in permeation of imiquimod from tape strips no. 2 to no. 12 is due to an increase in water content with *stratum corneum* depth which limits the permeation of imiquimod [61]. The poor water solubility and lipophilicity of imiquimod resulted in limited dermal permeation when the drug is applied to the skin as a topical cream. Specifically, as imiquimod is a lipophilic molecule, when the drug is only applied as a topical cream it is likely that the molecule mostly permeates from the cream and into the superficial layer of the *stratum corneum*. As the superficial layer of the *stratum corneum* are known to be lipid rich, imiquimod would partition into this lipid matrix and remain there relative to permeating deeper into the skin. This may serve as an explanation for the higher imiquimod ion intensity observed from tape strips obtained from skin samples treated with Aldara™ cream alone relative to skin subjected to microneedle application.

In contrast, it can be seen from **Figure 2 (b)** that perforating the skin with microneedles either before or after cream application results in a decrease in the measured imiquimod ion intensity from ToF-SIMS analysed tape strips in comparison to tape strips from skin samples treated with Aldara™ cream alone. This finding agrees with the trend observed from the HPLC results in **Figure 1 (b)** that showed lower imiquimod concentration in the pooled tape strips from skin samples subjected to microneedle perforation relative to Aldara™ cream only treated skins. This observation may be attributed to the generation of microneedle channels within the *stratum*

corneum with microneedle application. When the microneedle was applied as a pre-treatment using the 12 arrays via the poke-and-patch strategy, the *stratum corneum* is now perforated with aqueous microneedle channels. As the drug is poorly water soluble these aqueous channels may hinder the permeation of the drug into the *stratum corneum* resulting in lower imiquimod ion intensity relative to Aldara^{TM} cream. Without any aqueous microneedle channels in the cream only treated group, the drug will be able to partition and remain in the lipid rich matrix of the *stratum corneum*. However, when the microneedle was applied after cream application using either the 12 or 36 arrays, via the patch-and-poke strategy we also observed lower imiquimod ion intensity relative to Aldara^{TM} cream. In this instance, the microneedle application is now mechanically inserting the drug across the *stratum corneum* and directly into the epidermis and dermis. Therefore, there will be less cream available on the skin surface as evidenced from the HPLC data in **Figure 1 (a)** for skin wash. As there is less cream on the skin surface, there will now be less drug to partition from the skin surface and into the *stratum corneum* resulting in lower imiquimod ion intensity relative to Aldara^{TM} cream.

On the other hand, the current finding contradicts our previous report that showed higher imiquimod ion intensity from ToF-SIMS analysed tape strips obtained from the poke-and-patch approach relative to topical cream application alone [44]. In this work, a shorter microneedle length (250 μm) was employed while 1000 μm was used in this study. The shorter needles used in the previous work may generate shallower microneedle channels that remained mostly within the viable epidermis layer. These shallower microneedle pores are more likely to promote the permeation of imiquimod into the superficial layer of the skin rather than flowing deeper into the dermis. These shallower drug-filled microneedle channels may act as focal points for the drug to

radiate out to surrounding corneocytes, resulting in higher imiquimod intensity when a shorter microneedle length is used with the poke-and-patch approach relative to topical cream alone.

3.4 ToF-SIMS Analysis of Skin Cross-sections

3.4.1 Effect of microneedle pre-treatment "poke-and-patch" versus post-treatment "patch-and-poke" on the delivery of imiquimod.

It was apparent from ToF-SIMS analysis of tape strips as shown in **Figure 2 (b)**, that using either the poke-and-patch or patch-and-poke approach, we observed a similar trend in the permeation of imiquimod through the *stratum corneum*. This suggests that both microneedle application strategies, either before or after cream application may not influence the permeation of imiquimod through the *stratum corneum.* In order to investigate if the two solid microneedle application strategies may influence the intradermal delivery of imiquimod deeper into the skin, we employed ToF-SIMS analysis of skin cross-sections in addition to tape strip analysis. Understanding the spatial distribution of molecular species is paramount in elucidating the effectiveness of drug delivery systems within a biological tissue. Conventional liquid chromatography mass spectrometry (LC-MS) is traditionally employed to understand the effectiveness of a drug delivery strategy, however the extraction process employed leads to loss in spatial information [62]. ToF-SIMS has the capability to simultaneously map molecular ion of the dosed compound in tandem with the native fragment ions from skin tissue [38]. Examples of ion signals used to distinguish respective skin strata are $C_5H_{15}NPO_4^+$ (a fragment ion for phosphatidylcholine) and $C_{17}H_{32}N^+$ (a fragment ion for ceramide) [43]. The *stratum corneum* displays high levels of ceramide whilst being devoid of phospholipids [63]. Therefore, phosphatidylcholine ion fragments were used to map the

viable epidermis and dermis while ceramide fragment ions were used to identify the *stratum corneum*.

From **Figure 3**, it is evident that there is limited availability of imiquimod within deeper skin layers when applied either through topical cream alone **(i)** or via the poke-and-patch **(ii)** approach. However, when Aldara™ is applied via the patch-and-poke approach in **Figure 3 (iii)** and **(iv)**, we observed enhanced imiquimod delivery into the dermis. This observation agrees with the trend observed from the HPLC analysis from **Figure 1 (c)** that shows an increase in imiquimod concentration in the skin with the patch-and-poke approach using 36-needle array Dermapen®. In addition, the delivered drug is localised within microchannels formed during microneedle insertion. Typically nodular BCC presents 400 μm below the skin surface [13]. The ToF-SIMS analysis of skin cross-sections from **Figure 3** suggest that the patch-and-poke approach may be a suitable strategy to enable enhanced imiquimod delivery into the dermis for the treatment of nodular BCC.

It has been demonstrated previously that ToF-SIMS can chemically image drug permeation through microneedle channels in the *stratum corneum* and upper epidermis [44] . However, these studies adopted a poke-and-patch approach that showed localisation of imiquimod within the *stratum corneum* which agrees with the current findings [44]. One of the possible explanations for the limited drug permeation with the poke-and-patch approach is the viscoelastic property of the skin that causes some regions of the skin to recoil and close over time after microneedle application. In some instances, the closure can be as rapid as 5 minutes [64,65]. This rapid closure of microneedle pores may limit dermal permeation of imiquimod via the poke and patch approach. Additionally, perforating the skin with microneedles prior to cream application promotes the flow of more interstitial fluid into the microneedle channels. This results in the formation of hydrophilic

pores that act as a barrier to the entry of hydrophobic drugs, such as imiquimod, deeper into the dermis [46,47]. This phenomenon does not affect the intradermal delivery of imiquimod using the patch-and-poke approach, as the drug is mechanically driven into the skin during repeated microneedle insertion circumventing the effect of microneedle pore closure.

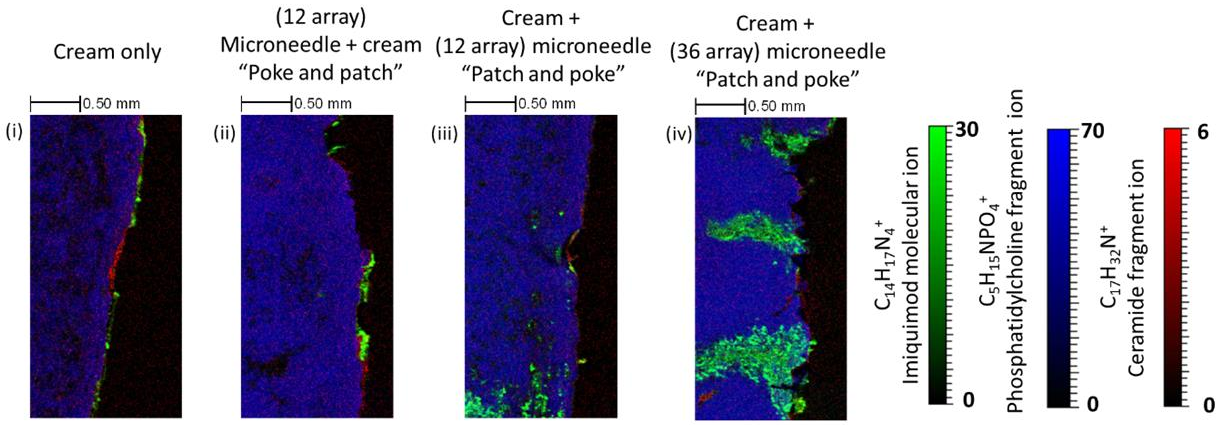

Figure 3. ToF-SIMS secondary ion distribution map of skin cross sections from porcine skin that were treated with (i) Aldara™ cream (5% w/w imiquimod) alone (ii) in combination with Dermapen (1000 µm) using the 'poke-and-patch' approach (iii)-(iv) in combination with Dermapen (1000 µm) using the 'patch-and-poke' approach with different needle arrays. This resulted in improved drug delivery into the lower layer of the skin (dermis) with the 'patch and poke' strategy.

Another possible limitation of the poke and patch approach with solid microneedles is limited drug flux from highly viscous formulations through microneedle perforated skin. This hypothesis was evaluated by Milewski *et al*. The group observed that as the viscosity of a formulation increases, the flux of naltrexone hydrochloride decreased across microneedle pretreated *ex vivo* mini-pig skin [66]. Pharmaceutical creams, such as Aldara™ (5% w/w imiquimod) are inherently viscous

formulations relative to gels and lotions [67]. The rapid closure of microneedle channels coupled with slow permeation of the drug from the highly viscous Aldara™ cream into the skin may only limit the drug distribution into the *stratum corneum* with the poke-and-patch approach.

Owing to the parallel detection capability, the ToF-SIMS data can simultaneously map the presence of excipients within biological tissues as well as the drug. One example of an excipient that is present in Aldara™ cream is isostearic acid. Conventionally, isostearic acid has been incorporated in various topical and cosmetic products as a permeation enhancer [68]. However, Walter *et al* have shown that isostearic acid also displayed active pharmacological properties which are independent of the immune mediated response induced by imiquimod [69]. Isostearic acid plays a critical role in inflammasome activation, which is pertinent for the overall efficacy of Aldara™ cream. It is also therefore of interest to chemically map the presence of isostearic acid in the microneedle channels. Through monitoring the molecular ion peak at *m/z* 285.3 indicated in **Figure 4 (a),** we were able to detect the co-localisation of the excipient within the microneedle channels as shown in **Figure 4 (b)** and **(c)**. The peak assignment for isostearic acid was validated by referring to fragmentation pattern at *m/z* 285 with the reference spectra of pure isostearic acid on silicon wafer as shown in the supplementary data (**Figure S3**).

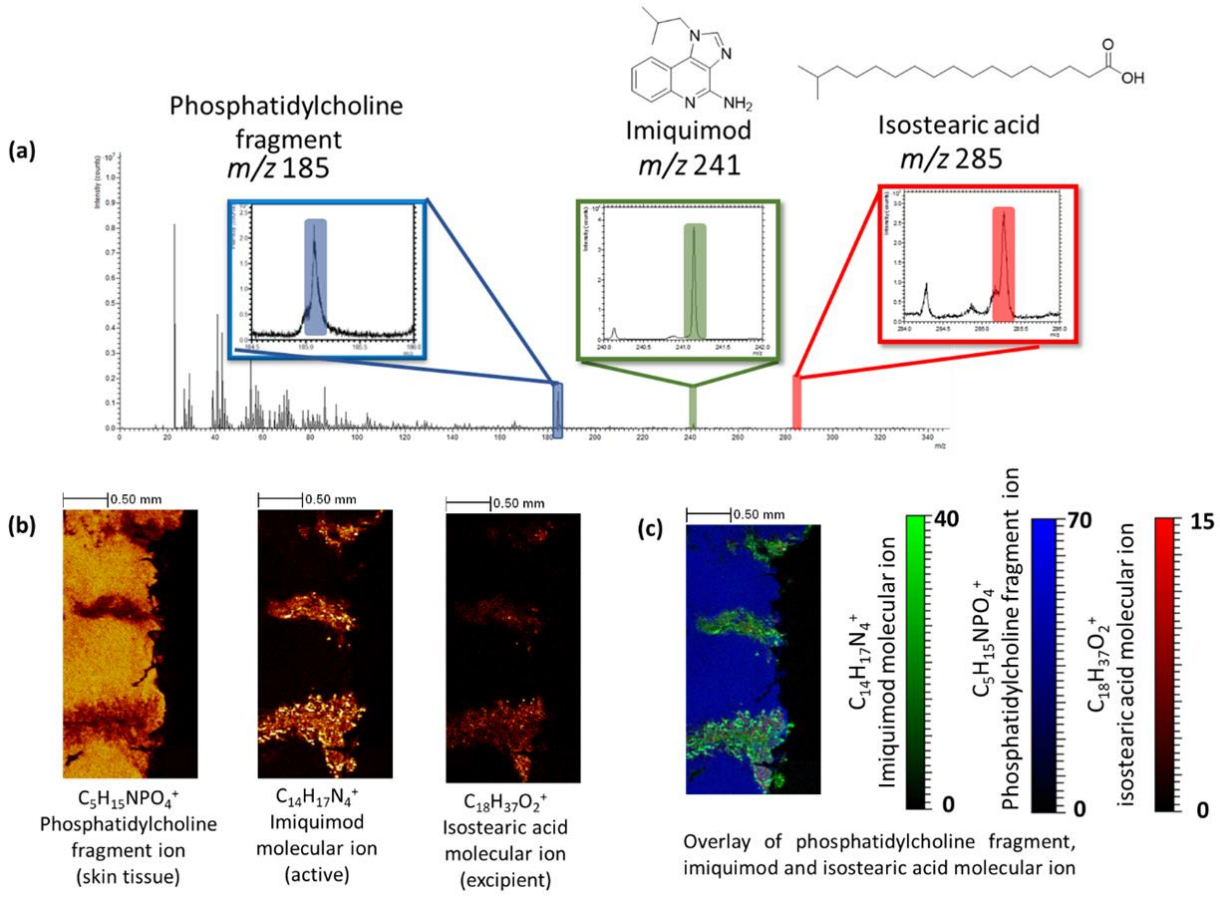

Figure 4. (a) Positive polarity ToF-SIMS spectra of *ex vivo* porcine skin treated with 5% w/w imiquimod topical cream using patch and poke approach, where the inset spectrum shows the peak of the $[M+H]^+$ of imiquimod at *m/z*=241 and $[M+H]^+$ of isostearic acid at *m/z*=285.3 (b) ToF-SIMS 2D chemical ion maps of phosphatidylcholine (biological tissue), imiquimod (active) and isostearic acid (excipient) acquired from cross section analysis of *ex vivo* porcine skin tissue after a 24 hour permeation experiment. Chemical ion map shows location of skin tissue along with the biodistribution of active and excipient. (c) an overlay image of the excipient isostearic acid marker ($C_{18}H_{37}O_2^+$) in red, imiquimod ($C_{14}H_{17}N_4^+$) in green and the skin marker ($C_5H_{15}NPO_4^+$) in blue. The overlay indicates the ability ToF-SIMS to detect the colocalisation of

imiquimod (active) and isostearic acid (excipient) within the microneedle channel within the *ex vivo* skin tissue.

Traditional methods to study microneedle-enhanced permeation require the use of fluorescently-labelled drug molecules to track the intradermal localisation of pharmaceuticals within the skin. This approach may alter the physiochemical properties of the drug leading to erroneous estimation of drug permeation into the skin [26]. In addition, such methods only allow the tracking of the active drug molecule which limits our understanding of the dermal distribution of the other components in the formulation such as polymers and fatty acid-based surfactants. The current work, highlights that the patch-and-poke strategy using oscillating solid microneedles may be a simple strategy to enable co-localised intradermal delivery of a poorly water soluble active and an excipient as evidenced by ToF-SIMS analysis. Similar to imiquimod, isostearic acid also has low water solubility which limits the penetration of the fatty acid into the more aqueous dermis [70]. The co-delivery of these compounds into the dermis ensures that isostearic acid may execute a synergistic action along with imiquimod in stimulating an effective inflammatory response for the treatment of nodular BCC.

3.4.2 Effect of vibration on the delivery of imiquimod into the dermis using patch-and-poke approach with Dermapen

One of the features of the Dermapen® is the vibration of microneedles at the tip of the device. This generates a stamp-like motion overcoming the issue of varying pressure of application by end-users [71]. Hence, we attempted to understand if vibration plays a functional role in the intradermal delivery of imiquimod using the patch and poke approach. We repeated the experiment using an *ex vivo* porcine skin permeation study followed by ToF-SIMS analysis of skin cross-section. As a comparator to the vibrating Dermapen®, we treated the skin with a Dermastamp™. The

Dermastamp™ perforates the skin in a single stamp motion without the assistance of a vibrating electric motor. Both microneedle devices used were 1000 µm in length. It can be seen from **Figure 5** that generation of imiquimod filled microneedle channels within the dermis with the patch-and-poke strategy only occurred when the skin was treated with the oscillating Dermapen® following cream application.

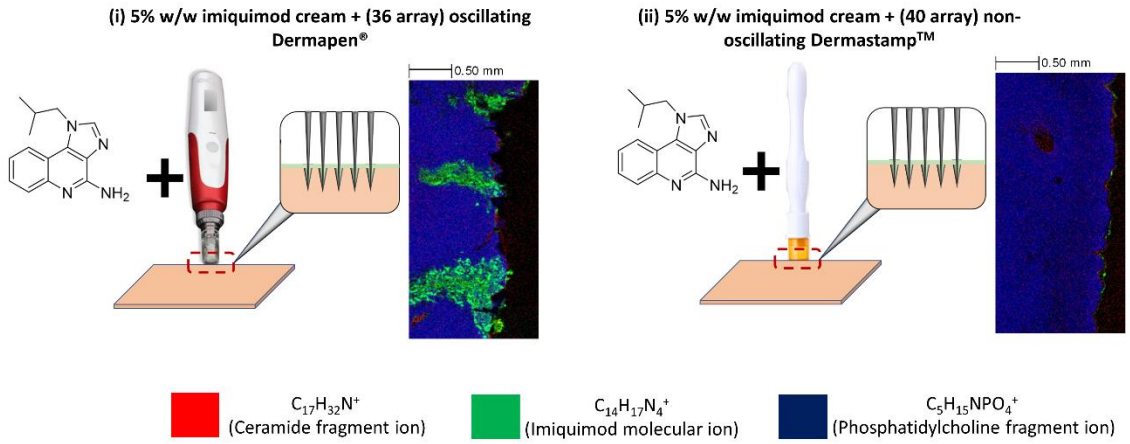

Figure 5. ToF-SIMS secondary ion distribution map of *skin* cross sections for *ex vivo* porcine skins that were treated with (i) Aldara cream (5% w/w imiquimod) followed by Dermapen® (1000 µm) application and (ii) Aldara cream (5% w/w imiquimod) application followed by 1000 µm Dermastamp™

The ability of the Dermapen® to efficiently penetrate the skin relative to other microneedle systems is attributed to the vibrating-stamping motion of the device during device application [72,73]. Izumi *et al* explored the effect of vibration on the penetration of microneedles into artificial silicone rubber skin. The group found that applying a vibration of 30 Hz to a microneedle array during skin insertion resulted in a reduction in the force needed to penetrate the skin [74]. The reduction in puncture force is attributed to the reduction in frictional forces experienced by microneedles under

vibration [75]. The rapid vibration of the microneedles also mitigates the likelihood of viscoelastic materials such as skin and topical cream from attaching to the microneedle during the insertion step. This phenomenon provides an explanation as to why the patch-and-poke motion using Dermastamp™ was unsuccessful in delivering imiquimod into the dermis. The topical cream along with superficial skin tissues (i.e. *stratum corneum*) may attach to the tip of the needles during microneedle application resulting in poor penetration profile. Aoyagi *et al* also showed that that vibration indeed plays a critical role in microneedle insertion. However, Aoyagi and co-workers also demonstrated that a reduction in puncture force is also achievable when the skin is stretched prior to microneedle application [76]. Unlike the Dermastamp™, the presence of shoulders at the tip of microneedle cartridge of the Dermapen® generates tension on the skin during microneedle application. This helps to reduce the propensity of the skin to fold around the needles while decreasing the puncture force needed to perforate the skin.

As it was apparent that the patch and poke approach using the Dermapen® provided the most effective intradermal delivery of imiquimod into skin, we then attempt to understand how imiquimod dermal distribution changes over 24 hours with this strategy. Subsequently, we repeated the *ex vivo* Franz cell permeation experiment using the patch-and-poke approach and performed ToF-SIMS analysis on the skin at five different time points. From **Figure 6**, we can see that using the patch-and-poke approach, the generation of imiquimod filled channels took place immediately (0 hours) post microneedle application on the skin after cream application. It is well known that the conventional poke-and-patch strategy is reliant on passive diffusion for the entry of drug molecules across aqueous microneedle channel to achieve intradermal delivery [66]. Such a process is both slow and ineffective for the delivery of hydrophobic molecules due to their poor solubility in the aqueous channels. Coupled with the rapid closure of microneedle channels, this

renders the poke-and-patch approach a poor strategy for the delivery of hydrophobic drugs. On the other hand, the patch-and-poke approach is dependent on the mechanical insertion of drug directly into the skin during microneedle application which overcomes the issues of solubility and pore closure.

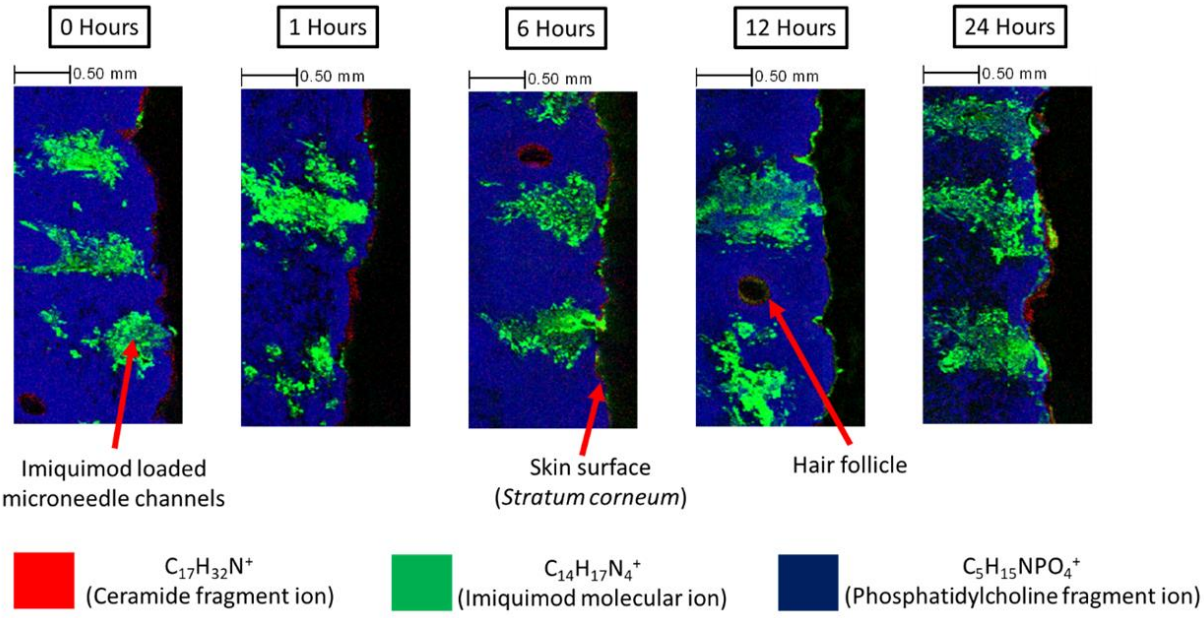

Figure 6. ToF-SIMS secondary ion distribution map of porcine skin cross sections from different time points. This highlights improved drug delivery into the lower layer of the skin (dermis) that persisted in the skin up to 24 hours. In addition, the formulation was immediately present in the deeper layers of the skin upon microneedle application. Phosphatidylcholine highlights the viable epidermis and dermis while ceramide highlights the top layer of the skin. Black circles indicate areas filled by hair follicles.

The presence of imiquimod loaded channels within the dermis that persisted for 24 hours was attributed to the poor water solubility of the drug [77]. The limited water solubility of imiquimod coupled with the fact that the water composition increases with dermal depth serves as possible explanation as to why imiquimod channels remained in the *ex vivo* skin tissues up to 24 hours [78]. The application of imiquimod cream followed by Dermapen® application generates localised

regions of imiquimod within the skin which resemble the structure of the microneedle channels. This shows that using a patch-and-poke strategy with oscillating microneedles provide an elegant synergy of existing products to enhance localisation of imiquimod intradermally. Such a drug delivery strategy may help prevent the requirement for surgical intervention for the treatment of deep-rooted basal cell carcinoma.

4. Conclusion

This work expands current understanding on the application of solid microneedles as a physical permeation enhancement strategy to promote the delivery of imiquimod into the skin for the treatment for BCC. The approach in which microneedles are used in combination with Aldara™ cream plays a critical role for the successful intradermal delivery of imiquimod into the skin. It has been demonstrated that in order to successfully deliver a hydrophobic molecule such as imiquimod into the dermis, a patch-and-poke approach is superior to the conventional poke-and-patch approach. Furthermore, it has also been demonstrated that an oscillating microneedle system, such as the Dermapen® for the patch-and-poke strategy, is a critical factor in providing successful intradermal delivery of imiquimod into the skin. Using this novel patch-and-poke approach hydrophobic drugs are mechanically inserted into the microneedle channels within the dermis upon microneedle application. This avoids the generation of hydrophilic/aqueous microneedle channels formed using the traditional poke-and-patch which can pose as a barrier to drug permeation. In summary, this work suggests that the combination of Aldara™ cream in combination with the oscillating Dermapen® provides an elegant synergy to enhance localised intradermal delivery of imiquimod. Such a strategy may provide a less invasive intervention to patients who would prefer an alternative treatment to surgery for the treatment of nodular BCC.

Supporting Information is available free of charge at the ACS website:-

Dye binding and histology study, HPLC analysis of imiquimod concentration in receptor fluid post-permeation study expressed as concentration (μg/ml), Isostearic acid peak assignment and validation.

Acknowledgements

This work was supported by the following funding: The University of Nottingham Centre for Doctoral Training in Advanced Therapeutics and Nanomedicine, Walgreens Boots Alliance and the EPSRC [grant number: EP/L01646X/1] via a PhD sponsorship for Akmal Sabri. We would like to thank Mr Zachary Cater (School of Engineering, University of Nottingham) for providing assistance in providing measurement for the microneedle dimensions.

Conflicts of interest: none.

References

(1) Prieto-Granada, C.; Rodriguez-Waitkus, P. Basal Cell Carcinoma: Epidemiology, Clinical and Histologic Features, and Basic Science Overview. *Curr. Probl. Cancer* **2015**, *39* (4), 198–205. https://doi.org/10.1016/j.currproblcancer.2015.07.004.

(2) Franchimont, C.; Pierard, G. E.; Cauwenberge, D. V. A. N. Episodic Progression and Regression of Basal Cell Carcinomas. *Br. J. Dermatol.* **1982**, *106*, 305–310.

(3) Kuijpers, D. I. M.; Thissen, M. R. T. M.; Neumann, M. H. A. Basal Cell Carcinoma: Treatment Options and Prognosis, a Scientific Approach to a Common Malignancy. *Am. J. Clin. Dermatol.* **2002**, *3* (4), 247–259.

(4) Crowson, A. N. Basal Cell Carcinoma : Biology , Morphology and Clinical Implications. *Mod. Pathol.* **2006**, *19* (S127–S147). https://doi.org/10.1038/modpathol.3800512.

(5) Colver, G. B. *Skin Cancer A Practical Guide to Management*, First.; Martin Dunitz Ltd, Ed.; Taylor & Francis: London, 2002.

(6) Goldenberg, G.; Golitz, L. .; Fitzpatrick, J. Histopathology of Skin Cancer. In *Managing Skin Cancer*; Stockfleth, E., Rosen, T., Schumaak, S., Eds.; Springer-Verlag Berlin Heidelberg: London, 2010; pp 17–35. https://doi.org/10.1007/978-3-540-79347-2.

(7) Coyle, M. J.; Takwale, A. Nonsurgical Management of Non-Melanoma Skin Cancer. In

Maxillofacial Surgery; Elsevier Inc., 2017; pp 761–764. https://doi.org/10.1016/B978-0-7020-6056-4.00055-1.

(8) Nijssen, A.; Bakker Schut, T. C.; Heule, F.; Caspers, P. J.; Hayes, D. P.; Neumann, M. H. A.; Puppels, G. J. Discriminating Basal Cell Carcinoma from Its Surrounding Tissue by Raman Spectroscopy. *J. Invest. Dermatol.* **2002**, *119* (1), 64–69. https://doi.org/10.1046/j.1523-1747.2002.01807.x.

(9) Goldenberg, G.; Hamid, O. Nonsurgical Treatment Options for Basal Cell Carcinoma - Focus on Advanced Disease. *J. Drugs Dermatol.* **2013**, *12* (12), 1369–1378.

(10) Lien, M. H.; Sondak, V. K. Nonsurgical Treatment Options for Basal Cell Carcinoma. *J. Skin Cancer* **2011**, *2011*, 571734. https://doi.org/10.1155/2011/571734.

(11) Tinelli, M.; Ozolins, M.; Bath-hextall, F.; Williams, H. C. What Determines Patient Preferences for Treating Low Risk Basal Cell Carcinoma When Comparing Surgery vs Imiquimod ? A Discrete Choice Experiment Survey from the SINS Trial. *BMC Dernatology* **2012**, *12*, 1–11. https://doi.org/10.1186/1471-5945-12-19.

(12) Jansen, M. H. E.; Mosterd, K.; Arits, A. H. M. M.; Roozeboom, M. H.; Sommer, A.; Essers, B. A. B.; Pelt, H. P. A. Van; Quaedvlieg, P. J. F.; Steijlen, P. M.; Nelemans, P. J.; et al. Five-Year Results of a Randomized Controlled Trial Comparing Effectiveness of Photodynamic Therapy , Topical Imiquimod , and Topical 5-Fluorouracil in Patients with Superficial Basal Cell Carcinoma. *J. Invest. Dermatol.* **2017**, *138* (3), 527–533. https://doi.org/10.1016/j.jid.2017.09.033.

(13) Williams, H. C.; Bath-Hextall, F.; Ozolins, M.; Armstrong, S. J.; Colver, G. B.; Perkins, W.; Miller, P. S. J. Surgery Versus 5% Imiquimod for Nodular and Superficial Basal Cell Carcinoma: 5-Year Results of the SINS Randomized Controlled Trial. *J. Invest. Dermatol.* **2017**, *137* (3), 614–619. https://doi.org/10.1016/j.jid.2016.10.019.

(14) Nakagawa, N.; Matsumoto, M.; Sakai, S. In Vivo Measurement of the Water Content in the Dermis by Confocal Raman Spectroscopy. *Ski. Res. Technol.* **2010**, *1* (20), 137–141. https://doi.org/10.1111/j.1600-0846.2009.00410.x.

(15) Yang, Y.; Sunoqrot, S.; Stowell, C.; Ji, J.; Lee, C.-W.; Kim, J. W.; Khan, S. A.; Hong, S. Effect of Size, Surface Charge, and Hydrophobicity of Poly(Amidoamine) Dendrimers on Their Skin Penetration. *Biomacromol* **2012**, *13*, 2154−2162. https://doi.org/10.1021/bm300545b.

(16) Kim, Y. C.; Park, J.-H.; Prausnitz, M. R. Microneedles for Drug and Vaccine Delivery. *Adv. Drug Deliv. Rev.* **2012**, *64* (14), 1547–1568. https://doi.org/10.1016/J.ADDR.2012.04.005.

(17) Donnelly, R. F.; Morrow, D. I. J.; McCarron, P. A.; Woolfson, A. D.; Morrissey, A.; Juzenas, P.; Juzeniene, A.; Iani, V.; McCarthy, H. O.; Moan, J. Microneedle-Mediated Intradermal Delivery of 5-Aminolevulinic Acid: Potential for Enhanced Topical Photodynamic Therapy. *J. Control. Release* **2008**, *129* (3), 154–162. https://doi.org/10.1016/j.jconrel.2008.05.002.

(18) Mikolajewska, P.; Donnelly, R. F.; Garland, M. J.; Morrow, D. I. J.; Singh, T. R. R.; Iani, V.; Moan, J.; Juzeniene, A. Microneedle Pre-Treatment of Human Skin Improves 5-Aminolevulininc Acid (ALA)- and 5-Aminolevulinic Acid Methyl Ester (MAL)-Induced PpIX Production for Topical Photodynamic Therapy without Increase in Pain or Erythema. *Pharm. Res.* **2010**, *27* (10), 2213–2220. https://doi.org/10.1007/s11095-010-0227-2.

(19) Donnelly, R. F.; Morrow, D. I. J.; McCarron, P. A.; David Woolfson, A.; Morrissey, A.; Juzenas, P.; Juzeniene, A.; Iani, V.; McCarthy, H. O.; Moan, J. Microneedle Arrays Permit Enhanced Intradermal Delivery of a Preformed Photosensitizer. *Photochem. Photobiol.* **2009**, *85* (1), 195–204. https://doi.org/10.1111/j.1751-1097.2008.00417.x.

(20) Zhang, J.; Wang, Y.; Jin, J. Y.; Degan, S.; Hall, R. P.; Boehm, R. D.; Jaipan, P.; Narayan, R. J. Use of Drawing Lithography-Fabricated Polyglycolic Acid Microneedles for Transdermal Delivery of Itraconazole to a Human Basal Cell Carcinoma Model Regenerated on Mice. *Jom* **2016**, *68* (4), 1128–1133. https://doi.org/10.1007/s11837-016-1841-1.

(21) Starr, N. J.; Abdul, K.; Wibawa, J.; Marlow, I.; Bell, M.; Pérez-garcía, L.; Barrett, D. A.; Scurr, D. J. Enhanced Vitamin C Skin Permeation from Supramolecular Hydrogels , Illustrated Using in Situ ToF-SIMS 3D Chemical Profiling. *Int. J. Pharm.* **2019**, *563* (October 2018), 21–29. https://doi.org/10.1016/j.ijpharm.2019.03.028.

(22) Wang, P. M.; Cornwell, M.; Hill, J.; Prausnitz, M. R. Precise Microinjection into Skin Using Hollow Microneedles. *J. Invest. Dermatol.* **2006**, *126* (5), 1080–1087. https://doi.org/10.1038/sj.jid.5700150.

(23) Ling, M. H.; Chen, M. C. Dissolving Polymer Microneedle Patches for Rapid and Efficient Transdermal Delivery of Insulin to Diabetic Rats. *Acta Biomater.* **2013**, *9* (11), 8952–8961. https://doi.org/10.1016/j.actbio.2013.06.029.

(24) Zhang, Y.; Jiang, G.; Yu, W.; Liu, D.; Xu, B. Microneedles Fabricated from Alginate and Maltose for Transdermal Delivery of Insulin on Diabetic Rats. *Mater. Sci. Eng. C* **2018**, *85* (December 2017), 18–26. https://doi.org/10.1016/j.msec.2017.12.006.

(25) Yu, W.; Jiang, G.; Zhang, Y.; Liu, D.; Xu, B.; Zhou, J. Polymer Microneedles Fabricated from Alginate and Hyaluronate for Transdermal Delivery of Insulin. *Mater. Sci. Eng. C* **2017**, *80*, 187–196. https://doi.org/10.1016/j.msec.2017.05.143.

(26) Vasquez, K. O.; Casavant, C.; Peterson, J. D. Quantitative Whole Body Biodistribution of Fluorescent- Labeled Agents by Non-Invasive Tomographic Imaging. *PLoS One* **2011**, *6* (6). https://doi.org/10.1371/journal.pone.0020594.

(27) Zhang, G.; Moore, D. J.; Sloan, K. B.; Flach, C. R.; Mendelsohn, R. Imaging the Prodrug-to-Drug Transformation of a 5-Fluorouracil Derivative in Skin by Confocal Raman Microscopy. *J. Invest. Dermatol.* **2007**, *127* (5), 1205–1209. https://doi.org/10.1038/sj.jid.5700690.

(28) Saar, B. G.; Contreras-Rojas, L. R.; Xie, X. S.; Guy, R. H. Imaging Drug Delivery to Skin with Stimulated Raman Scattering Microscopy. *Mol. Pharm.* **2011**, *8* (3), 969–975.

https://doi.org/10.1021/mp200122w.

(29) Förster, M.; Bolzinger, M. A.; Montagnac, G.; Briançon, S. Confocal Raman Microspectroscopy of the Skin. *Eur. J. Dermatology* **2011**, *21* (6), 851–863. https://doi.org/10.1684/ejd.2011.1494.

(30) Touboul, D.; Brunelle, A.; Laprévote, O. Improvement of Biological Time-of-Flight-Secondary Ion Mass Spectrometry Imaging with a Bismuth Cluster Ion Source. *J Am Soc Mass Spectrom* **2005**, *16*, 1608–1618. https://doi.org/10.1016/j.jasms.2005.06.005.

(31) Vandikas, M.; Hellström, E.; Malmberg, P.; Osmancevic, A. Imaging of Vitamin D in Psoriatic Skin Using Time-of- Flight Secondary Ion Mass Spectrometry (ToF-SIMS): A Pilot Case Study. *J. Steroid Biochem. Mol. Biol.* **2019**, *189* (October 2018), 154–160. https://doi.org/10.1016/j.jsbmb.2019.02.015.

(32) Oshima, S.; Kashihara, I.; Moritani, K.; Inui, N.; Mochiji, K. Soft-Sputtering of Insulin Films in Argon-Cluster Secondary Ion Mass Spectrometry. *Rapid Commun. Mass Spectrom.* **2011**, *25* (8), 1070–1074. https://doi.org/10.1002/rcm.4959.

(33) Denbigh, J. L.; Lockyer, N. P. ToF-SIMS as a Tool for Profiling Lipids in Cancer and Other Diseases. *Mater. Sci. Technol.* **2015**, *31* (2), 137–147. https://doi.org/10.1179/1743284714Y.0000000648.

(34) Park, J.-W.; Shon, H. K.; Yoo, B. C.; Kim, I. H.; Moon, D. W.; Lee, T. G. Differentiation between Human Normal Colon Mucosa and Colon Cancer Tissue Using ToF-SIMS Imaging Technique and Principal Component Analysis. *Appl. Surf. Sci.* **2008**, *255* (4), 1119–1122. https://doi.org/10.1016/j.apsusc.2008.05.102.

(35) Kulp, K. S.; Berman, E. S. F.; Knize, M. G.; Shattuck, D. L.; Nelson, E. J.; Wu, L.; Montgomery, J. L.; Felton, J. S.; Wu, K. J. Chemical and Biological Differentiation of Three Human Breast Cancer Cell Types Using Time-of-Flight Secondary Ion Mass Spectrometry. *Anal. Chem.* **2006**, *78* (11), 3651–3658. https://doi.org/10.1021/ac060054c.

(36) Baker, M. J.; Gazi, E.; Brown, M. D.; Clarke, N. W.; Vickerman, J. C.; Lockyer, N. P. ToF-SIMS PC-DFA Analysis of Prostate Cancer Cell Lines. *Appl. Surf. Sci.* **2008**, *255* (4), 1084–1087. https://doi.org/10.1016/j.apsusc.2008.05.256.

(37) Gazi, E.; Lockyer, N. P.; Vickerman, J. C.; Gardner, P.; Dwyer, J.; Hart, C. A.; Brown, M. D.; Clarke, N. W.; Miyan, J. Imaging ToF-SIMS and Synchrotron-Based FT-IR Microspectroscopic Studies of Prostate Cancer Cell Lines. *Appl. Surf. Sci.* **2004**, *231–232*, 452–456. https://doi.org/10.1016/j.apsusc.2004.03.170.

(38) Judd, A. M.; Scurr, D. J.; Heylings, J. R.; Wan, K.-W.; Moss, G. P. Distribution and Visualisation of Chlorhexidine Within the Skin Using ToF-SIMS: A Potential Platform for the Design of More Efficacious Skin Antiseptic Formulations. *Pharm. Res.* **2013**, *30* (7), 1896–1905. https://doi.org/10.1007/s11095-013-1032-5.

(39) Holmes, A. M.; Scurr, D. J.; Heylings, J. R.; Wan, K.; Moss, G. P. Dendrimer Pre-Treatment Enhances the Skin Permeation of Chlorhexidine Digluconate: Characterisation by in Vitro

Percutaneous Absorption Studies and Time-of-Flight Secondary Ion Mass Spectrometry. *Eur. J. Pharm. Sci.* **2017**, *104* (January), 90–101. https://doi.org/10.1016/j.ejps.2017.03.034.

(40) Čižinauskas, V.; Elie, N.; Brunelle, A.; Briedis, V. Skin Penetration Enhancement by Natural Oils for Dihydroquercetin Delivery. *Molecules* **2017**, *22* (9), 1536. https://doi.org/10.3390/molecules22091536.

(41) Kezutyte, T.; Desbenoit, N.; Brunelle, A.; Briedis, V. Studying the Penetration of Fatty Acids into Human Skin by Ex Vivo TOF-SIMS Imaging. *Biointerphases* **2013**, *8* (1), 3. https://doi.org/10.1186/1559-4106-8-3.

(42) Sjövall, P.; Skedung, L.; Gregoire, S.; Biganska, O.; Clément, F.; Luengo, G. S. Imaging the Distribution of Skin Lipids and Topically Applied Compounds in Human Skin Using Mass Spectrometry. *Sci. Rep.* **2018**, *8* (July), 1–14. https://doi.org/10.1038/s41598-018-34286-x.

(43) Sjövall, P.; Greve, T. M.; Clausen, S. K.; Moller, K.; Eirefelt, S.; Johansson, B.; Nielsen, K. T. Imaging of Distribution of Topically Applied Drug Molecules in Mouse Skin by Combination of Time-of-Flight Secondary Ion Mass Spectrometry and Scanning Electron Microscopy. *Anal. Chem.* **2014**, *86* (7), 3443–3452. https://doi.org/10.1021/ac403924w.

(44) Al-Mayahy, M. H.; Sabri, A. H.; Rutland, C. S.; Holmes, A.; McKenna, J.; Marlow, M.; Scurr, D. J. Insight into Imiquimod Skin Permeation and Increased Delivery Using Microneedle Pre-Treatment. *Eur. J. Pharm. Biopharm.* **2019**, *139* (February), 33–43. https://doi.org/10.1016/j.ejpb.2019.02.006.

(45) Mccaffrey, J.; Donnelly, R. F.; Mccarthy, H. O. Microneedles : An Innovative Platform for Gene Delivery. *Drug Deliv. Transl. Res.* **2015**, *5*, 424–437. https://doi.org/10.1007/s13346-015-0243-1.

(46) Badran, M. M.; Kuntsche, J.; Fahr, A. Skin Penetration Enhancement by a Microneedle Device (Dermaroller) in Vitro: Dependency on Needle Size and Applied Formulation. *Eur. J. Pharm. Sci.* **2009**, *36* (4–5), 511–523. https://doi.org/10.1016/j.ejps.2008.12.008.

(47) Gujjar, M.; Arbiser, J.; Coulon, R.; Banga, A. K. Localized Delivery of a Lipophilic Proteasome Inhibitor into Human Skin for Treatment of Psoriasis. *J. Drug Target.* **2015**, *2330*, 1–5. https://doi.org/10.3109/1061186X.2015.1087529.

(48) Benech-Kieffer, F.; Wegrich, P.; Schwarzenbach, R.; Klecak, G.; Weber, T.; Leclaire, J.; Schaefer, H. Percutaneous Absorption of Sunscreens in Vitro: Interspecies Comparison, Skin Models and Reproducibility Aspects. *Skin Pharmacol. Physiol.* **2000**, *13* (6), 324–335. https://doi.org/10.1159/000029940.

(49) Naguib, Y. W.; Kumar, A.; Cui, Z. The Effect of Microneedles on the Skin Permeability and Antitumor Activity of Topical 5-Fluorouracil. *Acta Pharm. Sin. B* **2014**, *4* (1), 94–99. https://doi.org/10.1016/j.apsb.2013.12.013.

(50) Davies, D. J.; Ward, R. J.; Heylings, J. R. Multi-Species Assessment of Electrical

Resistance as a Skin Integrity Marker for in Vitro Percutaneous Absorption Studies. *Toxicol. Vitr.* **2004**, *18* (3), 351–358. https://doi.org/10.1016/j.tiv.2003.10.004.

(51) Donnelly, R. F.; McCarron, P. A.; Zawislak, A. A.; David Woolfson, A. Design and Physicochemical Characterisation of a Bioadhesive Patch for Dose-Controlled Topical Delivery of Imiquimod. *Int. J. Pharm.* **2006**, *307* (2), 318–325. https://doi.org/10.1016/j.ijpharm.2005.10.023.

(52) Venturini, C. G.; Bruinsmann, F. A.; Contri, R. V.; Fonseca, F. N.; Frank, L. A.; D'Amore, C. M.; Raffin, R. P.; Buffon, A.; Pohlmann, A. R.; Guterres, S. S. Co-Encapsulation of Imiquimod and Copaiba Oil in Novel Nanostructured Systems: Promising Formulations against Skin Carcinoma. *Eur. J. Pharm. Sci.* **2015**, *79*, 36–43. https://doi.org/10.1016/j.ejps.2015.08.016.

(53) Sharma, M.; Sharma, G.; Singh, B.; Katare, O. P. Systematically Optimized Imiquimod-Loaded Novel Hybrid Vesicles by Employing Design of Experiment (DoE) Approach with Improved Biocompatibility, Stability, and Dermatokinetic Profile. *AAPS PharmSciTech* **2019**, *20* (4). https://doi.org/10.1208/s12249-019-1331-1.

(54) Paula, D. De; Martins, C. A.; Bentley, M. V. L. B. Development and Validation of HPLC Method for Imiquimod Determination in Skin Penetration Studies. *Biomed. Chromatogr.* **2008**, *22* (12), 1416–1423. https://doi.org/10.1002/bmc.1075.

(55) Donnelly, R. F.; Singh, T. R. R.; Morrow, D. I. J.; Woolfson, A. D. *Microneedle-Mediated Transdermal and Intradermal Drug Delivery*; John Wiley & Sons, Ltd: Chichester, UK, 2012. https://doi.org/10.1002/9781119959687.

(56) Stein, P.; Gogoll, K.; Tenzer, S.; Schild, H.; Stevanovic, S.; Langguth, P.; Radsak, M. P. Efficacy of Imiquimod-Based Transcutaneous Immunization Using a Nano-Dispersed Emulsion Gel Formulation. *PLoS One* **2014**, *9* (7), e102664. https://doi.org/10.1371/journal.pone.0102664.

(57) Maibach, H. I. Dermal Absorption Models in Toxicology and Pharmacology. *Clin. Toxicol.* **2007**, *45* (6), 736–736. https://doi.org/10.1080/15563650701502766.

(58) Banga, A. K. Microporation Applications for Enhancing Drug Delivery. *Expert Opin. Drug Deliv.* **2009**, *6* (4), 343–354. https://doi.org/10.1517/17425240902841935.

(59) Ng, S.-F.; Rouse, J. J.; Sanderson, F. D.; Meidan, V.; Eccleston, G. M. Validation of a Static Franz Diffusion Cell System for In Vitro Permeation Studies. *AAPS PharmSciTech* **2010**, *11* (3), 1432–1441. https://doi.org/10.1208/s12249-010-9522-9.

(60) Tranoulis, A.; Laios, A.; Mitsopoulos, V.; Lutchman-Singh, K.; Thomakos, N. Efficacy of 5% Imiquimod for the Treatment of Vaginal Intraepithelial Neoplasia—A Systematic Review of the Literature and a Meta-Analysis. *Eur. J. Obstet. Gynecol. Reprod. Biol.* **2017**, *218*, 129–136. https://doi.org/10.1016/j.ejogrb.2017.09.020.

(61) Johnsen, G. K.; Martinsen, Ø. G.; Grimnes, S. Estimation of In Vivo Water Content of the Stratum Corneum from Electrical Measurements. *Open Biomed. Eng. J.* **2009**, *3*, 8–12.

https://doi.org/10.2174/1874120700903010008.

(62) Porta Siegel, T.; Hamm, G.; Bunch, J.; Cappell, J.; Fletcher, J. S.; Schwamborn, K. Mass Spectrometry Imaging and Integration with Other Imaging Modalities for Greater Molecular Understanding of Biological Tissues. *Mol. Imaging Biol.* **2018**, *20* (6), 888–901. https://doi.org/10.1007/s11307-018-1267-y.

(63) Elias, P. M. Stratum Corneum Defensive Functions : An Integrated View. *J. Invest. Dermatol.* **2005**, *125* (2), 183–200. https://doi.org/10.1111/j.0022-202X.2005.23668.x.

(64) Bal, S.; Kruithof, A. C.; Liebl, H.; Tomerius, M.; Bouwstra, J.; Lademann, J.; Meinke, M. In Vivo Visualization of Microneedle Conduits in Human Skin Using Laser Scanning Microscopy. *Laser Phys. Lett.* **2010**, *7* (3), 242–246. https://doi.org/10.1002/lapl.200910134.

(65) Kalluri, H.; Banga, A. K. Formation and Closure of Microchannels in Skin Following Microporation. *Pharm. Res.* **2011**, *28* (1), 82–94. https://doi.org/10.1007/s11095-010-0122-x.

(66) Milewski, M.; Stinchcomb, A. L. Vehicle Composition Influence on the Microneedle-Enhanced Transdermal Flux of Naltrexone Hydrochloride. *Pharm Res* **2011**, *28*, 124–134. https://doi.org/10.1007/s11095-010-0191-x.

(67) Buhse, L.; Kolinski, R.; Westenberger, B.; Wokovich, A.; Spencer, J.; Chen, C. W.; Turujman, S.; Gautam-Basak, M.; Kang, G. J.; Kibbe, A.; et al. Topical Drug Classification. *Int. J. Pharm.* **2005**, *295* (1–2), 101–112. https://doi.org/10.1016/j.ijpharm.2005.01.032.

(68) Aungst, B. J. Structure/Effects Studies of Fatty Acid Isomers as Skin Penetration Enhancers and Skin Irritants. *Pharmaceutical Research*. 1989, pp 244–247. https://doi.org/10.1023/A:1015921702258.

(69) Walter, A.; Schäfer, M.; Cecconi, V.; Matter, C.; Urosevic-Maiwald, M.; Belloni, B.; Schönewolf, N.; Dummer, R.; Bloch, W.; Werner, S.; et al. Aldara Activates TLR7-Independent Immune Defence. *Nat. Commun.* **2013**, *4*, 1560. https://doi.org/10.1038/ncomms2566.

(70) Offeman, R. D.; Franqui-espiet, D.; Cline, J. L.; Robertson, G. H.; Orts, W. J. Extraction of Ethanol with Higher Carboxylic Acid Solvents and Their Toxicity to Yeast. *Sep. Purif. Technol.* **2010**, *72* (2), 180–185. https://doi.org/10.1016/j.seppur.2010.02.004.

(71) Zduńska, K.; Kołodziejczak, A.; Rotsztejn, H. Is Skin Microneedling a Good Alternative Method of Various Skin Defects Removal. *Dermatol. Ther.* **2018**, *31* (6), 1–8. https://doi.org/10.1111/dth.12714.

(72) Mccrudden, M. T. C.; Mcalister, E.; Courtenay, A. J.; Gonz??lez-V??zquez, P.; Raj Singh, T. R.; Donnelly, R. F. Microneedle Applications in Improving Skin Appearance. *Exp. Dermatol.* **2015**, *24* (8), 561–566. https://doi.org/10.1111/exd.12723.

(73) Singh, T. R. R.; Dunne, N. J.; Cunningham, E.; Donnelly, R. F. Review of Patents on Microneedle Applicators. *Recent Pat. Drug Deliv. Formul.* **2011**, *5* (1), 11–23.

https://doi.org/10.2174/187221111794109484.

(74) Izumi, H.; Yajima, T.; Aoyagi, S.; Tagawa, N.; Arai, Y.; Hirata, M.; Yorifuji, S. Combined Harpoonlike Jagged Microneedles Imitating Mosquito's Proboscis and Its Insertion Experiment with Vibration. *Electr. Eng. Japan* **2008**, *3* (4), 425–431. https://doi.org/10.1002/tee.20295.

(75) Yokoyama, Y.; Okabe, S. Reduction of Kinetic Friction by Harmonic Vibration in an Arbitrary Direction. *Bull. JSME-Japan Soc. Mech. Eng.* **1971**, *14* (68), 139–146.

(76) Aoyagi, S.; Izumi, H.; Fukuda, M. Biodegradable Polymer Needle with Various Tip Angles and Consideration on Insertion Mechanism of Mosquito's Proboscis. *Sensors Actuators A Phys.* **2008**, *143* (1), 20–28. https://doi.org/10.1016/j.sna.2007.06.007.

(77) Lin, W.; Hanson, S.; Han, W.; Zhang, X.; Yao, N.; Li, H.; Zhang, L.; Wang, C. Well-Defined Star Polymers for Co-Delivery of Plasmid DNA and Imiquimod to Dendritic Cells. *Acta Biomater.* **2017**, *48*, 378–389. https://doi.org/10.1016/j.actbio.2016.10.038.

(78) Egawa, M.; Arimoto, H.; Hirao, T.; Takahashi, M.; Ozaki, Y. Regional Difference of Water Content in Human Skin Studied by Diffuse-Reflectance near-Infrared Spectroscopy: Consideration of Measurement Depth. *Appl. Spectrosc.* **2006**, *60* (1), 24–28. https://doi.org/10.1366/000370206775382866.

For Table of Contents Only